

RSC Advances

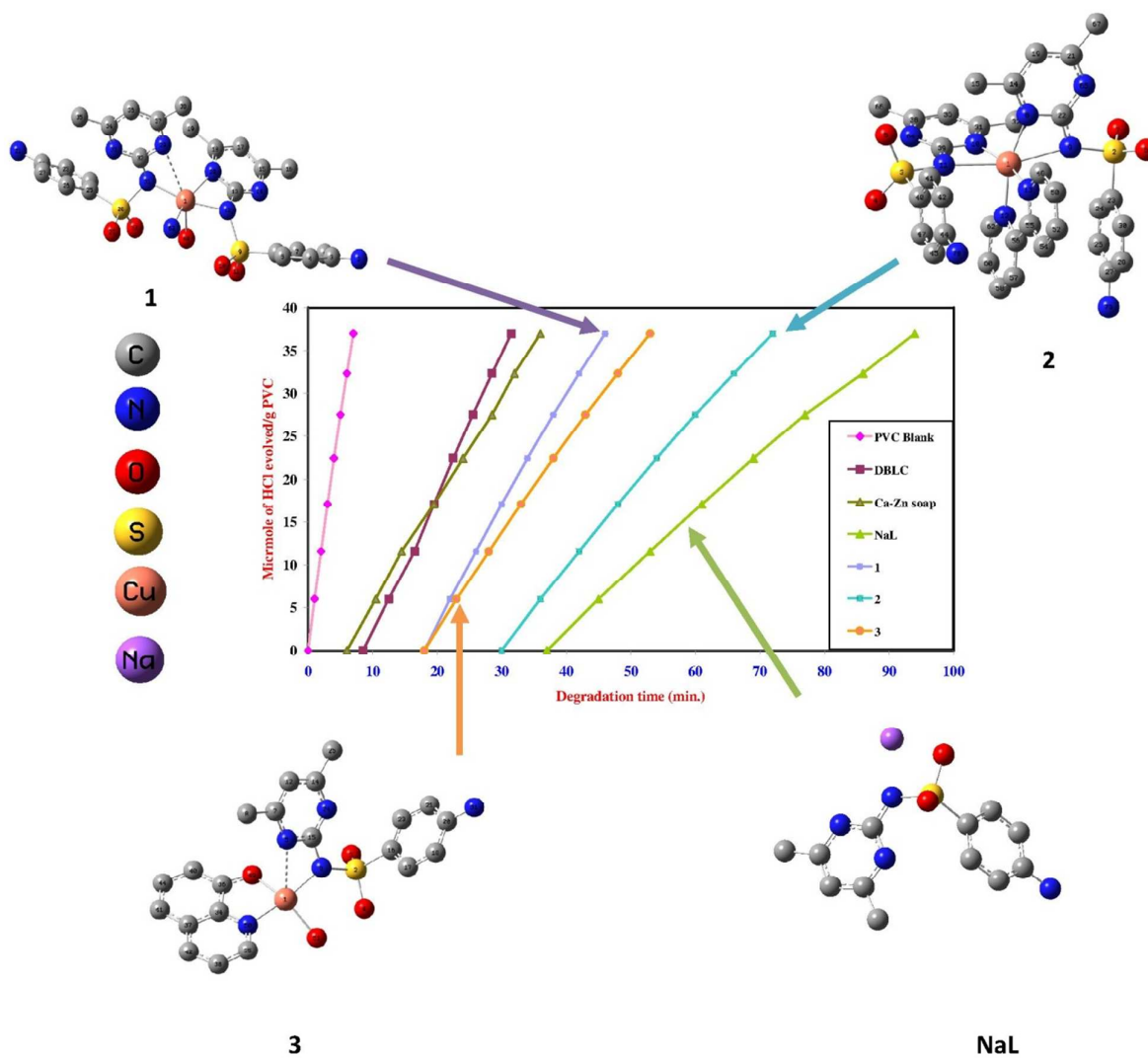


This is an *Accepted Manuscript*, which has been through the Royal Society of Chemistry peer review process and has been accepted for publication.

Accepted Manuscripts are published online shortly after acceptance, before technical editing, formatting and proof reading. Using this free service, authors can make their results available to the community, in citable form, before we publish the edited article. This *Accepted Manuscript* will be replaced by the edited, formatted and paginated article as soon as this is available.

You can find more information about *Accepted Manuscripts* in the [Information for Authors](#).

Please note that technical editing may introduce minor changes to the text and/or graphics, which may alter content. The journal's standard [Terms & Conditions](#) and the [Ethical guidelines](#) still apply. In no event shall the Royal Society of Chemistry be held responsible for any errors or omissions in this *Accepted Manuscript* or any consequences arising from the use of any information it contains.



Sulfamethazine copper(II) complexes as antimicrobial thermal stabilizer and co-stabilizers for rigid PVC: Spectroscopic, thermal, and DFT studies

Ahmed M. Mansour^{*}, Riham R. Mohamed

Chemistry Department, Faculty of Science, Cairo University, Gamaa Street, Giza 12613, Egypt

Abstract

[CuL₂(OH₂)]·1.5H₂O (**1**), [CuL₂(bpy)]·0.66H₂O (**2**) and [CuLQ(OH₂)]·H₂O (**3**) (HL = sulfamethazine, bpy = 2,2'-bipyridine and HQ = 8-hydroxyquinoline) complexes have been prepared, characterized (elemental analysis, IR, TGA, UV-Vis., magnetic and conductivity measurement), and tested for their antibacterial activity. Coordination of HL to Cu(II) ion did not markedly change its toxicity, but the presence of a secondary ligand gave rise to lower activity. Sulfamethazine and its complexes have been investigated as thermal stabilizers and co-stabilizers for the rigid PVC. A synergism has been achieved when the investigated compounds were mixed in equivalent weight ratio with the reference stabilizers. The experimental studies have been complemented by DFT data in terms of optimization, natural bond orbital analysis, and molecular electrostatic potential maps. Structural-thermal stabilization relationship showed that E_{HOMO}, ΔE, and softness are the most considerable descriptors for the correlation with the thermal stability.

Key Words: Sulfamethazine metal complexes; thermal stabilizer; synergistic effect; PVC; DFT; NBO

* Corresponding author, Tel.: +2 02 01222211253; Fax: +20 2 35728843. E-mail: inorganic_am@yahoo.com

1. Introduction

Metal complexes of sulfonamides have received great interest in the field of bioinorganic chemistry [1-3] as sulfonamides composed a vital class of the antimicrobial agents in the world owing to their low cost, and their ability to slow down the bacterial growth in the wounds or infected organs without appreciable toxicity to normal tissues. For example, zinc-sulfadiazine was used to prevent the bacterial infections in animals suffering from burns [2], while silver-sulfadiazine complex was applied in human topical burn therapy [3]. As reported, sulfonamides can interact with metal ions as mono-, bi- or tridentate ligand [4]. Sulfamethazine (HL) (Fig. 1) is a sulfa-based drug used as an antibacterial agent to treat diseases [5]. As well as other sulfonamides, HL presents a chemical structure that favors chemical modifications by means of complexation with some metal ions in order to initiate new complexes with more convenient antimicrobial properties [6]. Binuclear [Cu₂(CH₃COO)₂L₂]·2dmf and polymeric {[CuL₂]·2H₂O}_∞ complexes have been isolated, characterized, and their magnetic properties were discussed by Borrás et al. [7]. Recently, the crystal structures of octahedral Cu(II) [8], Zn(II), and

Cd(II) sulfamethazine [9], prepared from the acid form in presence of ammonia as a deprotonating agent, showed an important aspects in which the coordination sphere is formed from pyrimidic, and sulfonamidic N atoms of two sulfa molecules, water, and the terminal amino of a third sulfa molecule.

Poly(vinyl chloride) (PVC) was widely used in construction of materials, food package, decoration, medication and commodities (construction tubing, films and toys). Some attempts were performed to prepare antibacterial PVC composites to protect PVC from the bacteria or microbes during their daily usage as the addition of Zirconium phosphate containing nano Ag^+ [10] or TiO_2/Ag^+ nano-particles [11]. Besides, PVC undergoes extensive degradation during its molding and applications at higher T [12] come with an unacceptable discoloration, and a loss of its physical and mechanical properties together with a change in molecular weight [13]. Various kinds of thermal stabilizers were used to inhibit the degradation of PVC [14], but unfortunately the formed heavy metal chlorides as by-products will act as a catalyst for the subsequent dehydrochlorination of PVC [15]. Organic stabilizers have been studied as thermal stabilizer for PVC [16, 17]. A new trend has been established for use of thermal stabilizers of antimicrobial nature to obtain thermally stable antimicrobial PVC composites [16, 17].

In the present work, three Cu(II) complexes containing sulfamethazine as a primary ligand, and 2,2'-bipyridine, or 8-hydroxyquinoline as a secondary ligand were prepared (Fig. 2), and characterized, to assist in understanding of the modulation of the antibacterial behavior of HL upon complexation and/or presence of another ligand. Investigation of the studied compounds as thermally stable antimicrobial PVC composites has been explored. Molecular geometries, electronic structure [18, 19], natural bond orbital analysis, and molecular electrostatic potential maps have been discussed.

2. Experimental

2.1. Synthesis of complexes

Complex **1** [8] was prepared by dissolving 2 mmol of NaL (602 mg) with 1 mmol of $\text{CuSO}_4 \cdot 5\text{H}_2\text{O}$ (249 mg) in 20 mL water and the solution was heating to reflux for 2 h, where a brick-red complex was isolated, separated by filtration and washed with water. Complexes **2** and **3** were synthesized by adding 1 mmol of 2,2'-bipyridine (158 mg) or 8-hydroxyquinoline (146 mg) to 1 mmol aqueous solution of $\text{CuSO}_4 \cdot 5\text{H}_2\text{O}$, and the solution was gently heated until complete dissolution of the secondary ligand, and color change. Next, an aqueous solution of sodium sulfamethazine (2 mmol for **2**, and 1 mmol for **3**) was added and the resulting solution was refluxed for 4 h, where green and brown complexes were precipitated, respectively. The low molar conductance values indicate the non-electrolytic nature of the complexes [20]. Binary copper complexes of 2,2'-bipyridine, and 8-hydroxyquinoline were also for the

comparison with data of the new mixed-ligand complexes. The purity of the investigated compounds has been checked by TLC as a secondary determinant of purity.

- Data for **1**: Brick-red. Yield: 73%. Elemental analysis (%): calcd. $C_{24}H_{28}CuN_8O_5S_2 \cdot 1.5H_2O$: C 43.43, H 4.37, N 16.89, found: C 43.49, H 4.16, N 17.18. IR (cm^{-1}): 3538, $\nu(H_2O)$, 3360 $\nu(NH_2^{ss})$, 1625 $\nu(CN)_{py}$, 1591 $\nu(CN)_{py}$, 979 $\nu(SN)$, 675 $\nu(CS)$. MS: m/z : 619 [M^+]. UV-Vis. (DMF, nm): 295, 715. Molar Cond. (10^{-3} M, DMF, $\Omega^{-1}cm^2mol^{-1}$): 3.23. μ_{eff} (298 K, μ_B): 2.21.
- Data for **2**: Green. Yield: 89%. Elemental analysis (%): calcd. $C_{34}H_{34}CuN_{10}O_4S_2 \cdot 0.66H_2O$: C 51.89, H 4.49, N 17.80, found: C 52.76, H 4.17, N 18.46. IR (cm^{-1}): 3469 $\nu(NH_2^{ass})$, 3354 $\nu(NH_2^{ss})$, 1625 $\nu(C=N)_{py}$, 1603 $\nu(C=N)_{bpy}$, (1568, 1475, 1447) $\nu(C=C)_{py}$, 972 $\nu(SN)$, 676 $\nu(CS)$. MS: m/z : 789 [M^+]. UV-Vis. (DMF, nm): 300, 750. Molar Cond. (10^{-3} M, DMF, $\Omega^{-1}cm^2mol^{-1}$): 8.50. μ_{eff} (298 K, μ_B): 1.85.
- Data for **3**: Brown. Yield: 81%. Elemental analysis (%): calcd. $C_{21}H_{19}CuN_5O_3S \cdot H_2O$: C 50.14, H 4.21, N 13.92, found: C 49.72, H 4.12, N 15.88. IR (cm^{-1}): 3440 $\nu(NH_2^{ass})$, 3373 $\nu(NH_2^{ss})$, 1630 $\nu(C=N)_{py}$, 1593 $\nu(C=N)_{HQ}$, 1306 $\nu(C-O)_{HQ}$, 1498 $\nu(C=C)_{sulfa}$, 1461 $\nu(C=C)_{HQ}$, 1000 $\nu(SN)$, 674 $\nu(CS)$. MS: m/z : 522 [M^+]. UV-Vis. (DMF, nm): 295, 340, 411, 690. Molar Cond. (10^{-3} M, DMF, $\Omega^{-1}cm^2mol^{-1}$): 9.30. μ_{eff} (298 K, μ_B): 1.53.

2.2. Physical measurements

FT IR spectra were recorded as potassium bromide pellets using a Jasco FTIR 460 plus. The UV/Vis spectra were scanned on a Shimadzu Lambda 4B spectrophotometer. Elemental microanalysis was performed using Elementer Vario EL III. TGA was performed in N_2 atmosphere ($20 mL min^{-1}$) in a platinum crucible with a heating rate of $10 ^\circ C min^{-1}$ using a Shimadzu DTG-60H simultaneous DTG/TG apparatus. Magnetic measurements were carried out on a Sherwood scientific magnetic balance using Gouy method [21], and $Hg[Co(SCN)_4]$ as a calibrant. A digital Jenway 4310 conductivity meter (cell constant 1.02) was used for the determination of the molar conductance.

2.3. DFT calculations

The gas phase geometries of **1-3** were optimized without symmetry restrictions in the singlet state at DFT/B3LYP/LANL2DZ [22] level of theory using Gaussian 03 package [23]. Compounds **1-3** were characterized as local minima through harmonic frequency analysis. Electronic spectra were obtained by TD-DFT [18, 19]. Natural bond orbital analysis [24], molecular electrostatic potential maps [25] and the analysis of frontier molecular orbitals were performed at the same level of theory.

2.4. Method of evaluation of the stabilizing efficiency:

Samples of PVC (additive free, and $K = 70$, supplied by Hüls company-Germany) were prepared by mixing 1g of PVC powder with 2% weight of the stabilizer. Then, 0.2 g of the resulting fine powder was used in the study. Two methods have been used for the evaluation of the stabilizing efficiency of the studied compounds. The first method is measuring the induction period (T_s) using Congo-red dye paper, where its color changes from the red to blue once it meets the evolved HCl gas at 180°C in air [26]. The second way was achieved by potentiometrically measuring the dehydrochlorination rate at 180°C, in air (330 ml/min.) using digital pH meter type G 822 [27]. All the experiments were carried out in triplicate and the mean results are given. The extent of discoloration of PVC as a function of the degradation time was also determined by visually comparing the thermally degraded samples at various time intervals with the blank and the investigated reference thermal stabilizers.

2.5. Molecular mass determination by GPC

The average molecular mass of PVC was determined using *GPC-HPLC*, Waters 600 System controller, 717 plus auto-sampler. Columns: Phenomenx Phenogel 5 μm 50 A, 300 \times 7.8 mm. Detection: Waters model 2410 refractive index, ATTN = 16 \times Eluent: THF (100% by Vol.). Flow rate: 0.7 ml min^{-1} . Temperature: 50 °C. Injection volume: 25 μL .

Standards: Polystyrene 25,000, 13,000, 4,000, 2500, 200 g mol^{-1} (1.0 % m v^{-1}). Cubic fit calibration curve by Waters Millennium 32 GPC System Software. **Samples:** dissolved in THF at an approximate 1.0% m v^{-1} concentration.

2.6. Antibacterial activity

The antibacterial activity of compounds was tested on *Staphylococcus aureus* as a Gram-positive bacterium, and *Escherichia coli* as a Gram-negative bacterium according to a modified Kirby-Bauer disc diffusion method under standard conditions using Mueller-Hinton agar medium (tested for composition and pH), as previously reported [22].

3. Results and discussion

3.1. IR assignments

In order to clarify the bonding modes of sulfamethzine, bipyridine, and hydroxyquinoline in the reported complexes, the IR spectra of the free ligands, and their complexes were studied, and assigned on the basis of the careful comparison (Table S1†). The shifting of $\nu(\text{C}=\text{N})_{\text{py}}$ mode in **1** to lower wave number and the observation of two modes (1625 and 1591 cm^{-1}) indicates that the two sulfa ligands attached to the copper ion are not iso-energetically bound (discussed later). The presence of $\nu(\text{S}-\text{N})$ at

higher wave number (979 cm^{-1}), with respect to HL, supports the interaction of sulfonamidic N with metal ion. The $\nu_{\text{ss}}(\text{SO}_2)$ mode was found at the same position as NaL indicating that this group remains intact. The IR spectra of the complexes prepared from either the nitrate or sulphate salts are typical confirming that the anion of the metal salt has no role in the chelation. As shown in Table 1, the bands observed at 1638, 1625, and 972 cm^{-1} in **2** assigned to $\nu(\text{C}=\text{N})_{\text{bpy}}$, $\nu(\text{C}=\text{N})_{\text{py}}$ and $\nu(\text{S}-\text{N})$, respectively, suggesting the bidentate nature of HL and bpy. For **3**, the absence of $\nu(\text{OH})$, and the shifting of the $\nu(\text{C}=\text{N})_{\text{HQ}}$ to lower wave number (1593 cm^{-1}) confirming the mono-negatively bidentate nature of HQ ligand. The IR spectrum of **3** showed also two bands at 1630 and 1000 cm^{-1} assigned to $\nu(\text{C}=\text{N})_{\text{py}}$ and $\nu(\text{S}-\text{N})$ modes related to the involvement of sulfamethazine in the chelation through sulfonamidic and pyrimidic nitrogen atoms.

3.2. TGA/DTA

The thermal decomposition of **1** was accompanied by loss of 1.5 H_2O molecules, 4.26% (calcd. 4.06%) *via* two peaks at 47 and $80\text{ }^\circ\text{C}$. The TG curve of **2** exhibited a mass loss stage at $66\text{ }^\circ\text{C}$ assigned to desorption of $0.66\text{H}_2\text{O}$, 1.56% (calcd. 1.50%). Between $100\text{--}200\text{ }^\circ\text{C}$, complex **2** shows no weight loss. The degradations of **1** and **2** are incomplete in nitrogen atmosphere up to $1000\text{ }^\circ\text{C}$ reflecting their high stability [30] with overall mass loss amounts to 63.51 % and 83.08 %. The TG curve of **3** showed three main decomposition events. The 1st stage at $72\text{ }^\circ\text{C}$ is assigned to loss of one hydrated H_2O (found: 3.02%, calcd. 3.44%). The 2nd event (235 and $299\text{ }^\circ\text{C}$) is accompanied by elimination of NH_2phSO_2 , and pyrimidine moiety with a mass loss of 53.82% (calcd. 53.97%). The 3rd and 4th steps at 510 and $929\text{ }^\circ\text{C}$ bring the total mass loss up to 87.74% (calcd. 87.85%) expected for metallic copper as a final residue. Therefore, the presence of two sulfa ligands will increase the stability towards the thermal decomposition in the nitrogen atmosphere.

3.3. DFT studies

The optimization of **1** was constructed based on its crystallographic data [8] by taking into account that the terminal NH_2 group of a 3rd sulfa molecule is bonded to the metal ion. As shown in Fig. 2a, the Cu atom exhibits a distorted square-pyramidal geometry being coordinated to two sulfonamidic nitrogen atoms [$\text{Cu}-\text{N}12 = 2.098\text{ \AA}$, and $\text{Cu}-\text{N}31 = 2.050\text{ \AA}$], one pyrimidic [$\text{Cu}-\text{N}20 = 2.104\text{ \AA}$] of two sulfa molecules, water [$\text{Cu}-\text{O}40 = 2.184\text{ \AA}$], and terminal NH_2 [$\text{Cu}-\text{N}69 = 2.039\text{ \AA}$]. The value of the angular structural index parameter τ [31] is 0.15 characteristic of square-pyramidal stereochemistry. The pyrimidic N39 is close to Cu atom by 2.817 \AA . If this distance is short enough to be considered as Cu-N interaction, the coordination polyhedron around Cu can be considered as a highly distorted octahedral. In this case, it is worthy to note that while the Cu-N bond lengths of one sulfa ligand are

somewhat similar [Cu-N12 and Cu-N20], for the other molecule, one of the distances is longer than the other (Table S2). The difference between the four-member chelate angles of the two sulfa molecules [N12-Cu-N20 = 64.1 ° and N31-Cu-N39 = 53.8 °] and the axial angles [N20-Cu-N39 = 92.4 ° and N12-Cu-N39 = 118.4 °] are the causes of the distortion. Selected calculated bond lengths and angles are compared in Table S1†. A good agreement was found except the Cu-N69, which is largely deviated from the experimental value. This happens because the calculations were performed in gaseous state, whereas packing molecules with inter- and intra-molecular interactions are treated in the experimental measurements. According to NBO, the electronic arrangement of Cu^{II} is [Ar]4s^{0.27}3d^{9.34}4p^{0.42}5p^{0.01}, 10.029 valence and 0.010 Rydberg electrons with 28.034 total electrons leaving +0.9654 as a natural charge Cu atom. The occupancies of Cu 3d orbitals are as follows: $d_{xy}^{1.992}$ $d_{xz}^{1.977}$ $d_{yz}^{1.860}$ $d_{x^2-y^2}^{1.720}$ $d_{z^2}^{1.790}$.

Fig. 2b shows the optimized structure of [CuL₂(bpy)] (**2**) together with the labeling scheme used. Complex **2** contains a copper atom in a highly-symmetric octahedral geometry coordinated by four N atoms of two anionic bidentate sulfamethazine molecules, and two N atoms of a neutral 2,2' bipyridine ligand. The two covalent sulfonamidic bond distances are equal (2.437 Å), and longer than pyrimidic Cu-N bonds (2.033 Å). The bonds distances Cu-N_{bpy} (2.056 Å) are also equal. The electronic configuration of Cu atom is [Ar]4s^{0.27}3d^{9.33}4p^{0.41}5p^{0.01}, 17.994 core electrons, 10.009 valence electrons, and 0.01508 Rydberg electrons with 28.018 electrons as total electrons, which is in agreement with the calculated natural charge (+0.9817e) on copper atom. The occupancies of Cu 3d orbitals are as follows: $d_{xy}^{1.988}$ $d_{xz}^{1.992}$ $d_{yz}^{1.374}$ $d_{x^2-y^2}^{1.985}$ $d_{z^2}^{1.990}$.

A view of the optimized structure [CuLQ(OH₂)] (**3**) and its atom numbering are shown in Fig. 2c. The copper is four coordinated with N2O2 environment, coming from a bidentate N,O quinolinate ligand [CuN50 = 2.003 Å, Cu-O49 = 1.970 Å], sulfonamidic N6 [Cu-N6 = 1.988 Å] of an anionic sulfa drug, and water [Cu-O51 = 2.037 Å]. If the interaction of N5 atom with Cu (2.818 Å) is considered as a five bond, thus the structure is a highly distorted square-pyramidal ($\tau = 0.21$). The electronic arrangement of Cu^{II} is [Ar]4s^{0.29}3d^{9.35}4p^{0.32}, 17.995 core electrons, 9.950 valence, and 0.009 Rydberg electrons with 27.954 total electrons leaving +1.045 as natural charge on copper atom. The occupancies of Cu 3d orbitals are as follows: $d_{xy}^{1.826}$ $d_{xz}^{1.887}$ $d_{yz}^{1.952}$ $d_{x^2-y^2}^{1.699}$ $d_{z^2}^{1.981}$.

3.4. Electronic structure

Sulfonamides and their derivatives were characterized by a single absorption band at 260 nm [4]. The electronic spectrum of NaL showed two absorption bands in DMF at 260 and 276 nm [29].

Complex **1** displayed two absorption bands at 295, and 715 nm (Fig. S1) assigned to internal ligand transitions, and the unresolved ${}^2B_{1g} \rightarrow {}^2B_{2g}$, ${}^2B_{1g} \rightarrow {}^2A_{1g}$, and ${}^2B_{1g} \rightarrow {}^2E_{1g}$ transitions, in that order, in octahedral geometry, where the hexacoordinated environment is completed by a solvent and/or the terminal NH_2 of a third sulfa molecule [32]. The spectrum of **2** (Fig. S1†) showed a sharp band at 300 nm allocated to $\pi \rightarrow \pi^*$ of aromatic systems as well as a broad band at 750 nm assigned to a d-d transition in an octahedral geometry. The solution of HQ itself displayed two electronic transitions at 315 and 380 nm. Coordination of only HQ to Cu(II) gave rise to four bands at 290, 338, 412, and 595 nm (Fig. S1†). The broad band at 412 nm can be assigned to LMCT transition for the quinolate [33], while the band at 595 nm is attributed to a d-d transition. Complex **3** is characterized by four bands at 295, 340, 411, and 690 nm. Comparison between **3** and the binary complex suggested that the internal ligand transitions are established at 295 and 340 nm, LMCT from quinolate moiety is at 411 nm, and the unresolved d-d transitions can be considered at 690 nm in octahedral geometry.

This study was supported by TD-DFT calculations in the gas phase. In the model structures of **1-3**, to reduce the computer time, the aniline ring was replaced by a methyl group. Three absorption bands at 333, 481, and 631 nm with oscillator strengths of 0.0468, 0.0345, and 0.0051 are the features of **1**. The band at 631 nm is arising from H→L (HOMO: M and LUMO: L), which is actually $d_{yz} \rightarrow d_{x^2-y^2}$, (Fig. S2†) characterized to octahedral geometry. The band at 481 nm is allocated to H/H-1→L, while the transition at 333 nm is accounted for H-7→L [$\pi(\text{SO}_2) \rightarrow d_{x^2-y^2}$ LMCT]. The TD-DFT spectrum of **2** is composed of three transitions at 477, 516, and 817 nm assigned to H-2→L+1, H-3→L, and H-1→L. LUMO with β -spin is mainly of Cu $d_{x^2-y^2}$ character with contributions from π -bonding of bpy rings, whereas LUMO+1 is mainly of Cu d_{z^2} nature (Fig. 3). Therefore, The electronic transition at 817 nm is assigned to $d_{xz} \rightarrow d_{x^2-y^2}$. Assignments of the other transitions are as shown in Fig. 3. Complex **3** showed mainly three bands at 368, 513, and 772 nm assigned to H-5→L, H-1→L, and H-2/H-3→L as well as two shoulders at 374, and 461 nm allocated to H-3→L, and H-2→L/H→L+1, respectively. As shown in Fig. 4, the band at 368 nm characterizes the LMCT from the quinolate to Cu d_{z^2} , while this is at 461 nm is assigned to $\pi(\text{SO}_2)/\pi(\text{py})/\pi(\text{An}) \rightarrow d_{z^2}$ LMCT.

The observed effective magnetic moment values are 2.21, and 1.85 μ_B (298 K) for **1**, and **2** in that order. These values are in the acceptable range (1.60-2.20 μ_B) for the non-interacting magnetically diluted copper complexes [34]. Complex **3** shows a slightly low magnetic moment value (1.53 μ_B) that may indicate the copper centers are anti-ferromagnetically coupled to some extent [18].

3.5. Antibacterial activity

Sodium sulfamethazine and its complexes were screened *in vitro* for their antibacterial activity against *S. aureus* as Gram(+), and *E.coli* as Gram(-). Comparison to tetracycline as a standard was performed at the same conditions. NaL showed higher toxicity against *S. aureus* than *E.coli* that may be thought to be due to the different cell wall structure of the tested bacteria. Complex **1** is able to kill the microorganisms with a large inhibition zone with respect to NaL. It is well known that the actually active species of sulfamethazine drug is the ionic form. In other words, sulfamethazine penetrates the bacterial cells in the unionized form and once they enter a cell, their bacterial action would be due to its ionized form [35]. The increased activity of **1** can be explained by Tweed's chelation theory [36], which explicated that the lipophilicity of the organic ligand is changed by reducing of the polarizability of the M^{n+} ion *via* the L→M donation, and the possible electron delocalization over the complexes. Lipophilicity is related to membrane permeation in biological systems. Complex **1** may be also release the anionic form of sulfamethazine upon the entrance into the cell. In contrast, complexes **2** and **3** showed lower activity comparing with NaL and complex **1**. Complex **3** containing quinolate and one sulfa molecule is about triple times more active than the bpy **2** with two sulfa ligands. This behavior can be interpreted in terms of lipophilicity, stability, and the strength of the sulfonamidic Cu-N bonds, not in terms of the number of sulfa molecules per complex. The relationship between chelation, and bacterial toxicity is very complex, and other factors such as steric, electronic, diffusion, receptor sites, and pharmakinetik should be considered.

3.6. Thermal stabilization

3.6.1. Stabilization of thermally degraded rigid PVC

The results (Table S3†) of the thermal stabilization of rigid PVC stabilized by the studied compounds indicated the greater stabilizing efficiency of NaL, and its complexes compared with the reference compounds (DBLC and Cd-Ba-Zn stearates). This was indicated by the longer thermal stability periods (T_s) during which no detectable amounts of HCl are liberated. As shown in Fig. 5 (Table S4†), the stability value of NaL is almost seven times higher than those of the references. The efficiency is attributed to their radical potency, which interferes with the PVC radical degradation process. This most probably occurs not only through trapping of the radical species in the degradation process, but also by blocking the radical sites created on PVC chains.

3.6.2. Effect of mixed stabilizers

It became of interest to investigate the effect of mixing the investigated stabilizer together with those used in industry on the efficiency of stabilization in general. For this purpose, NaL was chosen for testing its efficiency as co-stabilizer. Mixing was done in the ranges of 0-100% of NaL relative to

the reference one. The total mixed stabilizer concentration was kept constant being 2 wt% based on the polymer weight. Results of the T_s value for each combination are tabulated in Table 2. As shown in Fig. 6 (Table S5†), a true synergism behavior was observed from the combination of NaL with any of the used reference stabilizers, irrespective of the class to which each reference stabilizer belongs. The maximum synergism was achieved, when NaL and either of the reference stabilizers were mixed in equimolar ratios (Table 1). The mixing process showed a slight improvement in the T_s (Fig. S3†, Table S6†). A remarkable improvement in the dehydrochlorination rate (after the thermal stability) of the thermally degraded rigid PVC as a result of mixing was observed (Fig. S4†, Table S7†). Thus, it seems that the different mechanisms by which both the investigated and the reference stabilizers work are beyond the obtained synergistic effect.

3.6.3. Elucidation of the molecular mass by GPC

GPC measurements were carried out for PVC before and after 30 min. of the thermal degradation process. The values of M_w , M_n and the polydispersity are presented in Table 2. Presence of the studied compounds results in a low decrease in the M_w values of PVC. A decrease in the M_w value of the blank PVC sample from 2.730×10^5 to 2.646×10^5 upon 30 min of thermal degradation was observed. After the time of degradation, the M_w of the PVC sample stabilized with NaL decreases from 2.730×10^5 to 2.612×10^5 . This confirms a good stabilizing effect of NaL, which decreases the extent of chain scission of PVC. Besides, the solubility test indicates the absence of gel formation reflecting the absence of the cross linking during the degradation. This is an evidence for the high efficiency of the investigated compounds, which can preserve both the mechanical and physical properties of the polymer.

3.6.4. Effect of mixed stabilizers on the extent of discoloration of thermally degraded PVC

The effect of mixing stabilizer NaL with DBLC and Cd-Ba-Zn stearate, in various weight ratios, on the degree of discoloration of thermally degraded rigid PVC is shown in Table 3. All the samples were heated at 180 °C, in air, for 60 min. All the mixed stabilizers exhibit a lower extent of discoloration than the reference stabilizer, rather than the investigated stabilizers when they are used alone. In all cases, the sample treated with 1:1 weight ratio of the investigated and reference stabilizers showed the least degree of discoloration and consequently the better color stability. This confirms the synergistic effect between their modes of action.

3.6.5. TGA for stabilized and non-stabilized PVC

Thermogravimetric data for the non-stabilized and stabilized PVC with the investigated stabilizers are shown in Table 4. The investigated stabilizers improved the thermal stability of PVC, as the initial

decomposition temperature of PVC stabilized with NaL, and complexes **1-3** was recorded at 240, 275, 270, and 262 °C, respectively, comparing with the unstabilized one, 180 °C. Moreover, the unstabilized PVC lost 44% of its mass at 300°C with respect to the stabilized one with NaL (58%), and complex **2** (42%). At 350°C, the unstabilized PVC lost 61% of its mass, while PVC stabilized with NaL lost 65% of its mass and PVC stabilized with **2** lost 60 %. From the previously mentioned results, it was clear that all stabilizers above 250 °C their degradation rate is higher than PVC.

3.7. Structure-thermal stabilization relationship

The crucial aim of structure-thermal stabilization relationship is to correlate the induction period (T_s) of the reported compounds with different quantum chemical descriptors such as E_{HOMO} , E_{LUMO} , energy gap, ionization energy, electron affinity, dipole moment, hardness, and softness. Energies and compositions of frontier molecular orbitals [18, 25] are important parameters in several chemical and pharmacological processes. E_{HOMO} is associated with the electron donating ability, while E_{LUMO} indicates the ability of the molecule to accept electrons. A good correlation ($R^2 = 0.9998$) was found between T_s and E_{HOMO} , where the stability of PVC increases (except **3**) as E_{HOMO} decreases. ΔE can decide whether the molecule is hard or soft. Soft molecule is more polarizable than the hard one. It was found that NaL, the most significantly stabilizer compound here, has the highest ΔE and lowest dipole moment values (Table S4†). The chemical hardness and softness of a molecule are good indicators for the chemical reactivity of a given molecule. The order of the softness is $NaL < \mathbf{1} < \mathbf{2} < \mathbf{3}$ suggesting that a hard compound has a highest stabilization performance.

Molecular electrostatic potential (MEP) map [24] is used for qualitative explanation of electrophilic or nucleophilic attack as well as H-bond interactions, and defines regions of local negative and positive potential in the molecule. As shown in Fig. 7, NaL molecule is covered by region of zero potential. For **1** and **3**, the main contribution to the strong positive charge region is coming from the metal center, while a region of zero potential is spreading all over the remaining area. In case of **2**, a positive area is located over the metal, and the contribution to the negative region is pending on the bipyridine residue. Therefore, presence of zero potential areas will increase the thermal stability of the PVC.

4. Conclusion

Structural studies of binary and ternary Cu(II) complexes of sulfamethazine antibacterial drug have been studied both experimentally and theoretically and are correlated here. Complex **3** containing quinolate and one sulfa molecule is three times more toxic, as antibacterial agent, than the bipyridine **2** with two sulfa ligands. This may be interpreted in terms of lipophilicity, stability, and the strength of

the sulfonamidic Cu-N bonds, not in terms of the number of sulfa molecules per complex. Investigation of the studied compounds as thermally stable antimicrobial PVC composites has been also explored. A good stabilization effect of the free drug was observed, which can preserve both the mechanical and physical properties of the polymer by decreasing the extent of the chain scission of PVC and prevents the gel formation. The free ligand was chosen also for testing its efficiency as co-stabilizer. Mixing the investigated stabilizers with any of the reference stabilizers leads to a remarkable improvement both in the T_s value and in lowering the extent of discoloration, reaching its maximum at equivalent weight ratio of investigated stabilizer to reference one. Structural thermal stabilization relationship showed that E_{HOMO} , energy gap, softness, and MEP maps were the most significant descriptors for correlating the molecular structures of the studied compounds and their thermal stabilization performance

5. References:

- [1] S. Roland, R. Ferone, R.J. Harvey, V.L. Styles, R.W. Morrison, *J. Biol. Chem.* 1979, **254**, 10337.
- [2] (a) N.C. Baenziger, S.L. Modak, C.L. Fox, *Acta Crystallogr.* 1983, **C39**, 1620; (b) C.J. Brown, D.S. Cook, L. Sengier, *Acta Crystallogr.* 1985, **C41**, 718.
- [3] (a) N.C. Baenziger, A.W. Struss, *Inorg. Chem.* 1976, **15**, 1807; (b) D.S. Cook, M.F. Turner, *J. Chem. Soc., Perkin Trans.* 1975, **2**, 1021.
- [4] A.M. Mansour, *Inorg. Chim. Acta* 2013, **394**, 436.
- [5] F. de Zayas-Blanco, M.S. García-Falcón, J. Simal-Gándara, *Food. Contr.* 2004, **15**, 375.
- [6] G.M. Golzar Hossain, Syntheses and structural studies of metal complexes of sulfa drugs. PhD Thesis, Cardiff University, 2005.
- [7] L. Gutierrez, G. Alzuet, J. Borrás, A. Castineiras, A. Rodriguez-Forteza, E. Ruiz, *Inorg. Chem.* 2001, **40**, 3089.
- [8] J.B. Tommasino, F.N.R. Renaud, D. Luneau, G. Pilet, *Polyhedron* 2011, **30**, 1663.
- [9] A. García-Raso, J.J. Fiol, S. Rigo, A. López-López, E. Molins, E. Espinosa, E. Borrás, G. Alzuet, J. Borrás, A. Castiñeiras, *Polyhedron* 2000, **19**, 991.
- [10] X. Chen, C. Li, L. Zhang, S. Xu, Q. Zhou, Y. Zhu, X. Qu, *China Particuol* 2004, **2**, 226.
- [11] Q. Cheng, C. Li, V. Pavlinek, P. Saha, H. Wang, *Appl. Surf. Sci.* 2006, **252**, 4154.
- [12] I.C. McNeill, L. Memetea, W.J. Cole, *Polym. Degrad. Stab.* 1995, **49**, 181.
- [13] (a) K. Patel, A. Velazquez, H.S. Calderon, G.R. Brown, *J. Appl. Polym. Sci.* 1992, **46**, 179, (b) J.P.H.M. Hillemans, C.M.C.J. Colemonts, R.J. Meier, B.J. Kip, *Polym. Degrad. Stab.* 1993, **42**, 323, (c) R.J. Meier, B.J. Kip, *Polym. Degrad. Stab.* 1992, **38**, 69.

- [14] (a) R.D. Dworkin, *J. Vinyl Technol.* 1989, **11**, 15, (b) G.Y. Levai, G.Y. Ocskay, Z.S. Nyitrai, *Polym. Degrad. Stab.* 1994, **43**, 159.
- [15] (a) J.F. Rabek, J. Lucki, H. Kereszti, T. Hjertberg, Q.B. Jun, *J. Appl. Polym. Sci.* 1990, **39**, 1569, (b) W.H. Cheng, Y.C. Liang, *J. Appl. Polym. Sci.* 2000, **77**, 2464.
- [16] M.W. Sabaa, S.T. Rabie, R.R. Mohamed, *J. Therm. Anal. Calorim.* 2012, **109**, 1503.
- [17] M.M. Fahmy, R.R. Mohamed, *Molecules* 2012, **17**, 2927.
- [18] A.M. Mansour, *Inorg. Chim. Acta* 2013, **408**, 186.
- [19] N.T. Abdel-Ghani, A.M. Mansour, *J. Coord. Chem.*, 2012, **65(5)**, 763.
- [20] J. Pons, A. Chadghan, J. Casabó, A. Alvarez-Larena, J. Francesc Piniella, J. Ros, *Polyhedron* 2001, **20**, 2531.
- [21] N.T. Abdel-Ghani, M.F. Abo El-Ghar, A.M. Mansour, *Spectrochim. Acta A* 2013, **104**, 134.
- [22] (a) N.T. Abdel-Ghani, A.M. Mansour, *Eur. J. Med. Chem.* 2012, **47**, 399, (b) N.T. Abdel-Ghani, A.M. Mansour, *Inorg. Chim. Acta* 2011, **373**, 249.
- [23] M.J. Frisch, G.W. Trucks, H.B. Schlegel, G.E. Scuseria, M.A. Robb, J.R. Cheeseman, V.G. Zakrzewski, J.A. Montgomery, R.E. Stratmann, J.C. Burant, S. Dapprich, J.M. Millam, A.D. Daniels, K.N. Kudin, M.C. Strain, O. Farkas, J. Tomasi, V. Barone, M. Cossi, R. Cammi, B. Mennucci, C. Pomelli, C. Adamo, S. Clifford, J. Ochterski, G.A. Petersson, P.Y. Ayala, Q. Cui, K. Morokuma, D.K. Malick, A.D. Rabuck, K. Raghavachari, J.B. Foresman, J. Cioslowski, J.V. Ortiz, A.G. Baboul, B.B. Stefanov, G. Liu, A. Liashenko, P. Piskorz, I. Komaromi, R. Gomperts, R.L. Martin, D.J. Fox, T. Keith, M.A. Al-Laham, C.Y. Peng, A. Nanayakkara, C. Gonzalez, M. Challacombe, P.M.W. Gill, B. G. Johnson, W. Chen, M.W. Wong, J.L. Andres, M. Head-Gordon, E.S. Replogle, J.A. Pople, GAUSSIAN 03 (Revision A.9), Gaussian, Inc., Pittsburgh, 2003.
- [24] A.E. Reed, L.A. Curtius, F. Weinhold, *Chem. Rev.* 1988, **88**, 899.
- [25] A.M. Mansour, *Spectrochim. Acta A*, 2014, **123**, 257.
- [26] ASTM D 4202-92. Test Method of Thermal Stability of Poly (Vinyl Chloride) (PVC) Resin (Withdrawn 1998).
- [27] Z. Vymazal, E. Czako, B. Meissner, J. Stepek, *J. Appl. Polym. Sci.* 1974, **18**, 2861.
- [28] G.M. Golzar Hossain, A.J. Amoroso, A. Banu, K.M.A. Malik, *Polyhedron* 2007, **26**, 967.
- [29] A.M. Mansour, *J. Mol. Struct.* 2013, **1035**, 114.
- [30] (a) G. Faraglia, F. Barbaro, S. Sitran, *Transition Met. Chem.*, 1990, **15**, 242-245, (b) N.T. Abdel-Ghani, A.M. Mansour, *J. Mol. Struct.* 2011, **991**, 108-126.

- [31] (a) J. Pons, A. Chadghan, J. Casabo, A. Alvarez-Larena, J.F. Piniella, J. Ros. *Polyhedron*, 2001, **20**, 2531, (b) A.M. Mansour, *J. Coord. Chem.*, 2012, **66(7)**, 1118.
- [32] (a) C. Fernandes, A. Neves, A.J. Bortoluzzi, A.S. Mangrich, E. Rentschler, B. Szpoganicz, E. Schwingel, *Inorg. Chim. Acta* 2001, **320**, 12, (b) D.H. Lee, Narasimha, N. Murthy, K.D. Karlin, *Inorg. Chem.* 1997, **36**, 5785.
- [33] G. Psomas, A. Tarushi, E.K. Efthimiadou, Y. Sanakis, C.P. Raptopoulou, N. Katsaros, *J. Inorg. Biochem.* 2006, **100**, 1764.
- [34] A. Cotton, G. Wilkinson, advanced Inorganic Chemistry, 2nd Ed. 1972.
- [35] W.O. Foye, T.L. Lemke, D.A. Williams, Principles of medicinal Chemistry, 4th ed., Williams & Williams 1995, pp 709-713.
- [36] B. Tweedy, *Phytopathology* 1964, **55**, 910.

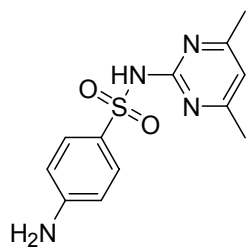


Fig. 1: Structure of sulfamethazine ligand (HL) utilized in this work.

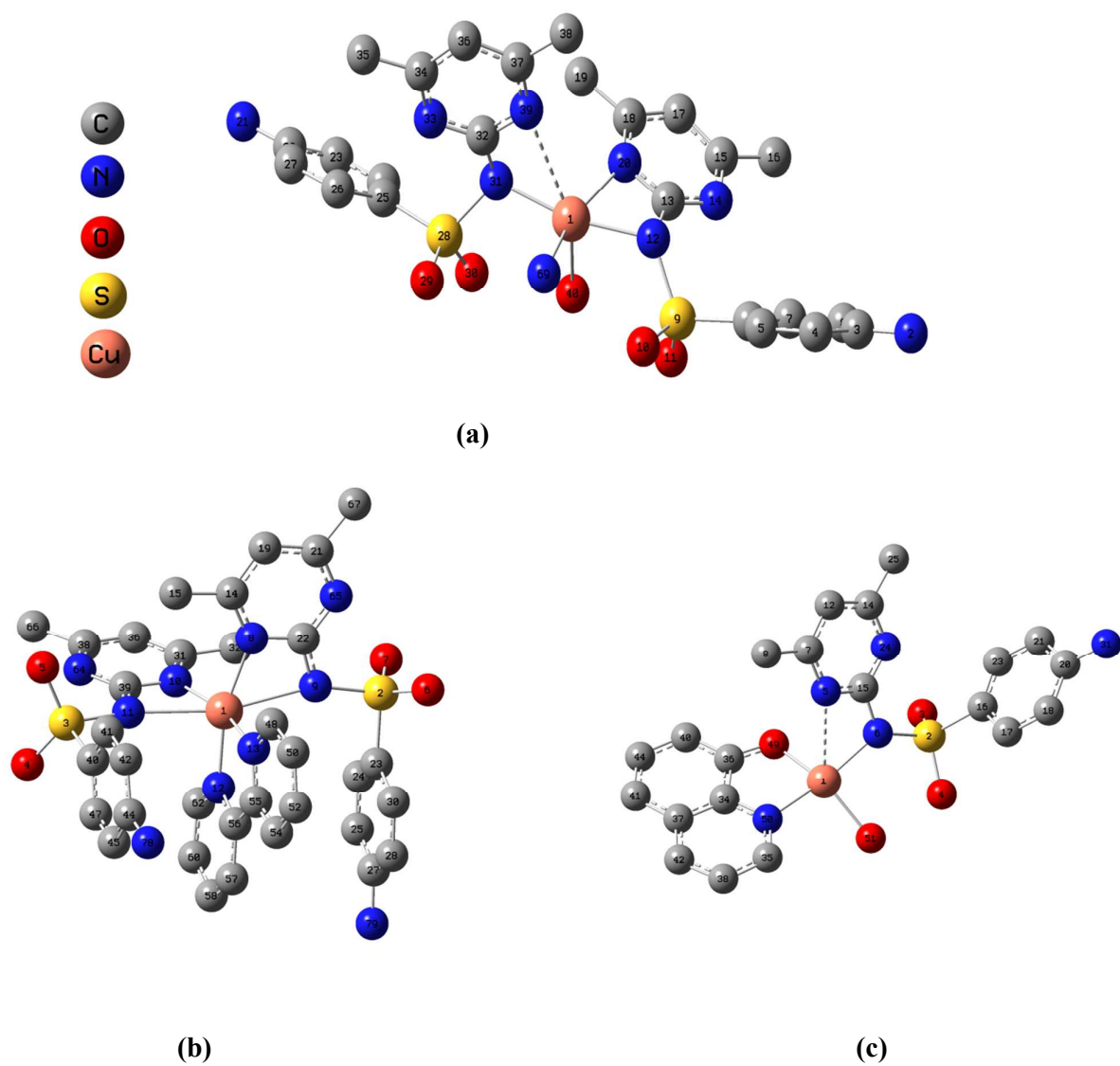


Fig. 2: Local minimum structures of complexes a) **1**, b) **2**, and c) **3** obtained at the B3LYP/LANL2DZ level of theory.

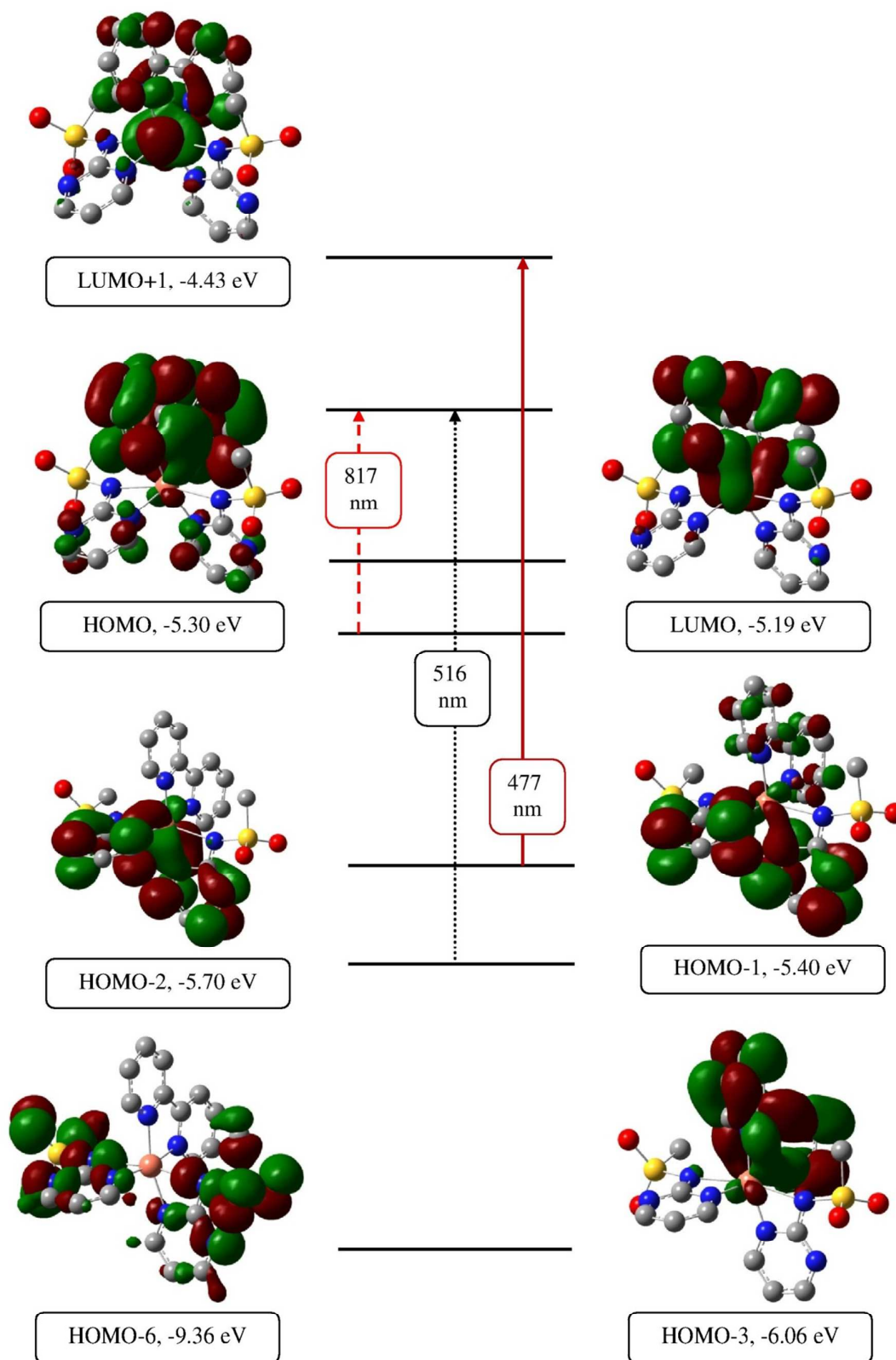


Fig. 3: TDDFT-calculated electronic transitions in complex 2.

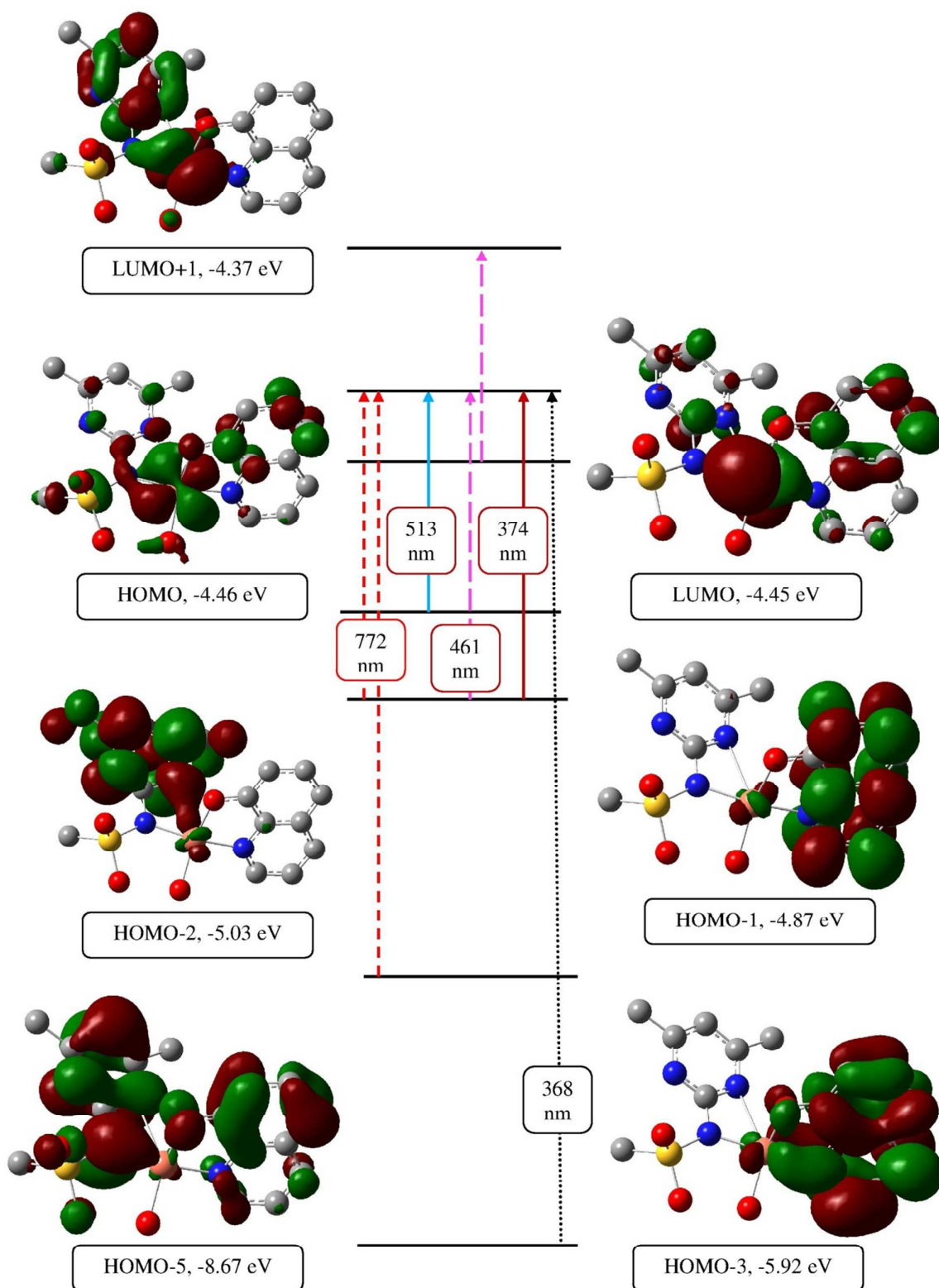


Fig. 4: TDDFT-calculated electronic transitions in complex 3.

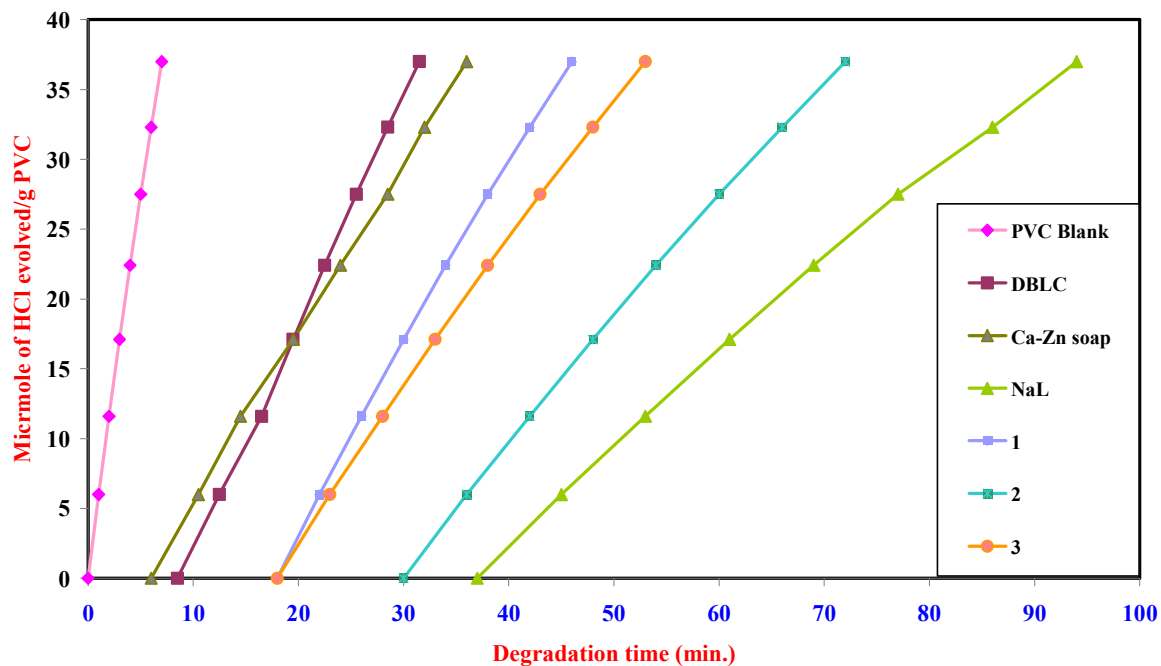


Fig. 5: Dehydrochlorination rate of PVC blank, PVC stabilized with reference stabilizers and the investigated stabilizers. All experiments were carried out in triplicate and the mean results are given.

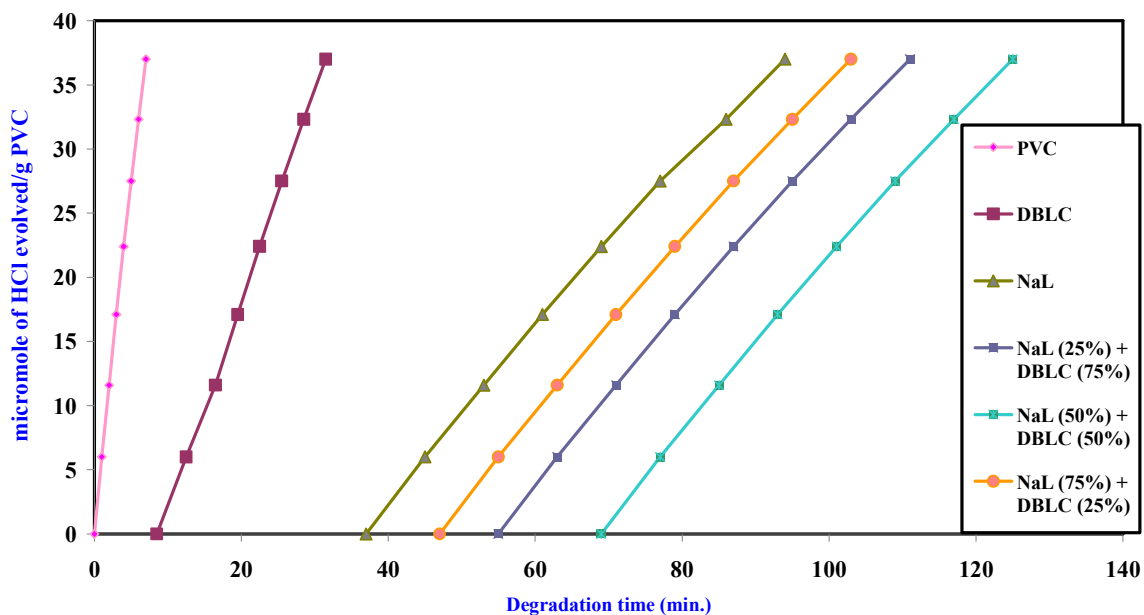


Fig. 6: Dehydrochlorination rate of PVC blank, PVC stabilized with DBLC and the investigated stabilizer (NaL) in different ratios. All experiments were carried out in triplicate and the mean results are given.

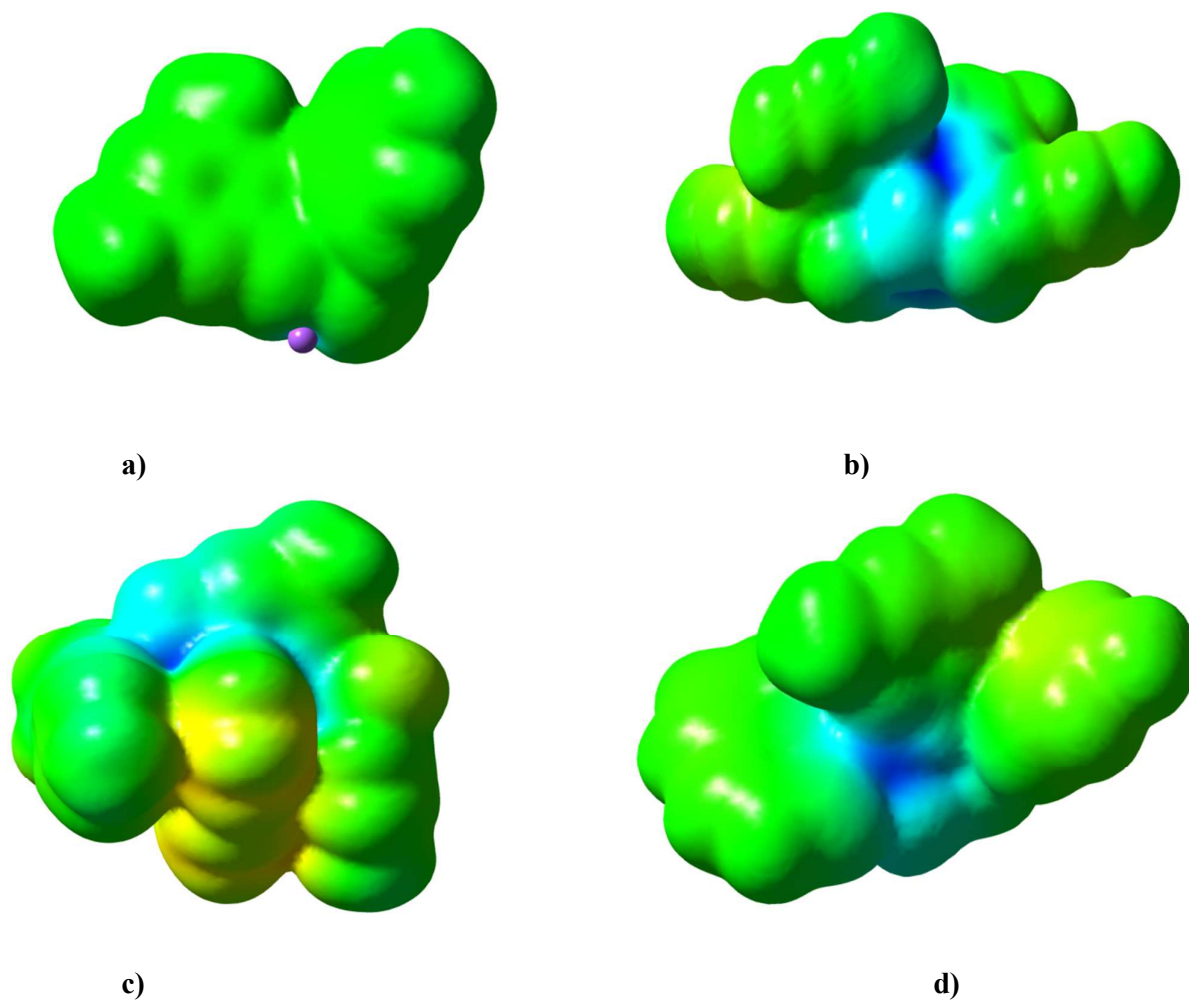


Fig. 7: Molecular electrostatic potential of complexes a) NaL, b) **1**, c) **2**, and d) **3**. The electron density isosurface is 0.004 a.u.

Table 1. Effect of mixing stabilizers of NaL on the thermal stability (T_s).











Compound mixing ratio	Induction time (min)*
NaL (25%) : DBLC (75%)	60
NaL (50%) : DBLC (50%)	74
NaL (75%) : DBLC (25%)	52
NaL (25%) :Ca-Zn stearate(75%)	56
NaL (50%) :Ca-Zn stearate(50%)	60
NaL (75%) :Ca-Zn stearate(25%)	52

* The overall mixed stabilizers concentration was kept constant at 2 mass % of PVC.

Table 2: GPC measurements of degraded PVC samples:

Sample	Degradation Time (min.)	M_w (g/mol) $\times 10^4$	M_n (g/mol) $\times 10^4$	PD
PVC (Blank)	0	27.30	11.9	2.294
PVC	30	26.46	9.943	2.662
PVC + NaL	30	26.12	10.483	2.492

Table 3. Effect of mixing NaL with reference stabilizers on the discoloration of thermally degraded rigid PVC at 180 °C, in air, for 60 min.

Weight ratio NaL: DBLC	color	Weight ratio NaL: Ca-Zn Stearate	color
100/0		100/0	
75/25		75/25	
50/50		50/50	
25/75		25/75	
0/100		0/100	

The overall mixed stabilizers concentration was kept constant at 2 mass % of PVC.

Table 4: TG data for PVC blank and PVC stabilized with the investigated stabilizers.

T (°C)	PVC	PVC + NaL	PVC + 2	PVC+ 3	PVC+ 1
Initial Decomposition Temperature (IDT)	180°C	240°C	270°C	262°C	275°C
T (°C)	Mass loss % of PVC	Mass loss % of PVC + NaL	Mass loss % of PVC + 2	Mass loss % of PVC + 3	Mass loss % of PVC + 1
200	5	0	0	0	0
250	11	22	0	0	0
280	32	52	20	15	20
300	44	58	42	40	42
350	61	65	60	60	60
400	62	63	65	62	65